Passivated Iron as Core−Shell Nanoparticles

E. E. Carpenter,* S. Calvin, R. M. Stroud, and V. G. Harris

Naval Research Laboratory, Washington, D.C. 20375

Received March 7, 2003
Revised Manuscript Received May 27, 2003

The properties of nanometer-sized magnetic particles of iron have been studied extensively both experimentally and theoretically. Although these particles show promise for practical applications such as catalysis, magnetic recording, magnetic fluids, and biomedical applications, their utility has been limited due to uncontrolled oxidation. One method for controlling the oxidation is to coat the particles, creating a core−shell structure. This core−shell structure maintains the favorable magnetic properties of metallic iron while protecting the nanoparticle from oxidation.

Using reverse micelles as reaction vessels, it is possible to synthesize iron nanoparticles that are coated with a native oxide shell.[1−3] Using the aqueous cores of reverse micelles allows for rapid homogeneous nucleation, while the micellar diffusion maintains slow particle growth.[4] The micellar factors play an important role in determining the particle size. Carrying out the reaction in a sequential fashion allows for the product of the first step to act as a nucleation site for the second passivating shell formation.[5]

A 0.4 M surfactant solution is prepared with NP4 and NP7 (w/w = 0.25) with the cyclohexane. NP4 and NP7 are commercially available nonylphenol poly(ethoxylate) ethers sold by Rhodia under the name Igepal CO-430 and CO-610. The two different chain lengths are used for additional stabilization of the micelle region.[6] The aqueous metal solution and a reducing solution are made by dissolving 0.3 g of $FeCl_2 \cdot 4H_2O$ in 1.6 mL of H_2O and 0.2 g of $NaBH_4$ in 1.6 mL of H_2O, respectively.[7] Micelle solutions are prepared by adding 50 mL of the surfactant solution to both the metal solution and the reducing solution.[2] The metal containing micelle solution is added to a 500-mL three-necked flask and degassed under flowing nitrogen, while the reducing solution is degassed using an ultrasonic bath for 5 min. The reducing solution is added rapidly to the reaction flask under magnetic stirring. The reaction solution turns black immediately with evolution of hydrogen gas.

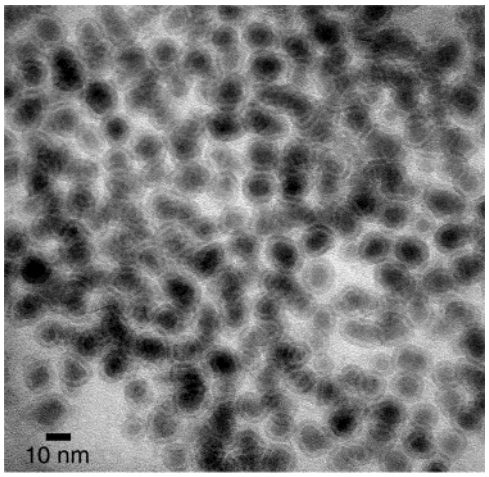

Figure 1. Bright-field transmission electron micrograph of Fe/iron oxide core−shell particles. The metallic cores average 6.1 nm in diameter and the oxide shell averages 2.7 nm in thickness, giving a total average particle size of 11.5 nm.

An additional reducing micelle solution is prepared in the same fashion to form the coating. This micelle solution is formed by dissolving 0.2 g of $NiCl_2 \cdot 6H_2O$ in 1.8 mL of H_2O with 50 mL of surfactant solution. After the iron has reacted for 45 min, the second reducing solution is added, followed rapidly by the second metal solution. The reaction is allowed to continue for 5 min before the reaction is quenched using 200 mL of degassed methanol. The passivated magnetic nanoparticles are removed from the reaction mixture using magnetic separation. The particles are washed using additional methanol to ensure the complete removal of the surfactant, unreacted cations, and uncoated particles.

The core−shell structure of the particles was characterized by transmission electron microscopy (TEM). The particles (see Figure 1) consist of metallic cores, having an average diameter of 6.1 nm, surrounded by an oxide shell, averaging 2.7 nm in thickness, for a total average particle diameter of 11.5 nm. Elemental analysis determined by XAS, EDS, and ICP-OES determined the nickel and boron concentrations to be <4 at. %. The nickel is present to aid in the formation of the passivating layer. While others[8,9] have found the presence of stoichiometric iron borides from sodium borohydride reduction of ferrous salts, we find evidence to suggest the present of iron-rich metallic glass, the small amount of boron present most likely located on the surface of the growing particle[8] and results in disorder in the iron core. This is not entirely surprising since conditions exist with rapid aqueous reduction of iron without a large excess of sodium borohydride for the preferential formation of metallic iron over the formation of the iron borides.[2] An analysis of the X-ray absorption near-edge

(1) Glavee, G. N.; Klabunde, K. J.; Sorensen, C. M.; Hadjipanayis, G. C. *Langmuir* **1993**, *9*, 162−169.
(2) Glavee, G. N.; Klabunde, K. J.; Sorensen, C. M.; Hadjipanayis, G. C. *Inorg. Chem.* **1995**, *34*, 28−35.
(3) Glavee, G. N.; Klabunde, K. J.; Sorensen, C. M.; Hadjipanayis, G. C. *Inorg. Chem.* **1993**, *32*, 474−477.
(4) Ingelsten, H. H.; Bagwe, R.; Palmqvist, A.; Skoglundh, M.; Svanberg, C.; Holmberg, K.; Shah, D. O. *J. Colloid Interface Sci.* **2001**, *241*, 104−111.
(5) Carpenter, E. E.; Kumbhar, A.; Wiemann, J. A.; Srikanth, H.; Wiggins, J.; Zhou, W. L.; O'Connor, C. J. *Mater. Sci. Eng. A* **2000**, *286*, 81−86.
(6) Zhong, Q.; Steinhurst, D. A.; Carpenter, E. E.; Owrutsky, J. C. *Langmuir* **2002**, *18*, 7401−7408.
(7) Iron(II) chloride, nickel(II) chloride, and sodium borohydride were purchased from Alfa Aesar. Cyclohexane was purchased from GFS Chemicals and nonylphenol poly(ethoxylate) 4 and 7 (NP) were obtained from Rhodia Chemicals (Igepal CO-430 and CO-610).
(8) Duxin, N.; Stephan, O.; Petit, C.; Bonville, P.; Colliex, C.; Pileni, M. P. *Chem. Mater.* **1997**, *9*, 2096−2100.
(9) Duxin, N.; Pileni, M. P.; Wernsdorfer, W.; Barbara, B.; Benoit, A.; Mailly, D. *Langmuir* **2000**, *16*, 11−14.

10.1021/cm034131l CCC: $25.00 © 2003 American Chemical Society
Published on Web 07/30/2003

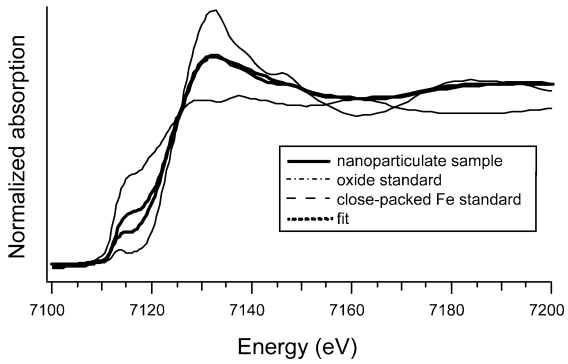

Figure 2. Comparison of X-ray absorption spectra for the core/shell sample to bulk standards. The fit is a linear combination of the standard spectra in the ratio 48% oxide to 52% close-packed iron.

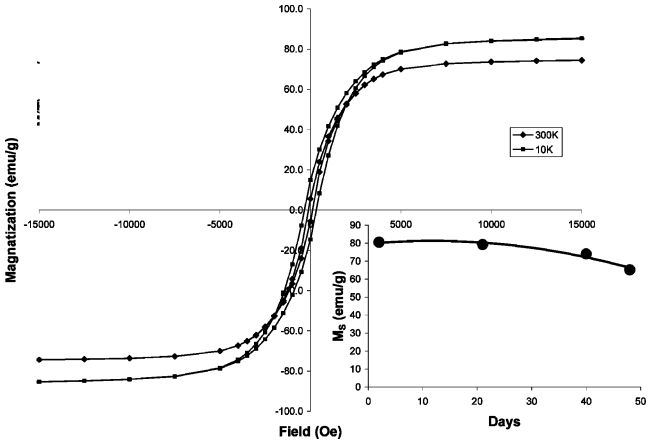

Figure 3. Magnetization versus field plot at 300 and 10 K. The inset on the lower right corner represents the change in the M_S values as a function of days.

structure (XANES) and the extended X-ray absorption fine structure (EXAFS)[10] indicated that ≈50% of the iron in the sample was present as a low boron content amorphous metallic glass, with the remainder in the form of a disordered oxide phase. The structures suggested by the EXAFS analysis were confirmed by comparison to the spectra of standards. To simulate the disordered oxide of the shell, a mixture of iron oxides was used.[11] Permalloy ($Ni_{0.8}Fe_{0.2}$) was used as a standard for the iron glass since in materials the Fe exists in a moderately disordered environment based on close-packed symmetry. The normalized spectra of these materials were then combined in the ratio suggested by the EXAFS and XANES fits. The result is shown in Figure 2. The close match confirms a composition in which approximately 50% of the iron atoms are in a nearly close-packed metallic phase, with the remainder being in an oxide. Although some previous studies have suggested passivating iron oxides may be highly disordered spinels,[12] they generally appear, as here, amorphous in EXAFS spectra.[13]

Magnetic characterization was performed using a Quantum Design MPMS-5S magnetometer (SQUID detector). Samples were prepared as dried powders placed in gelatin capsules and stored on a benchtop exposed to atmospheric conditions to allow for oxidation. Magnetization versus applied field curves, measured at 300 and 10 K, are presented in Figure 3. At 300 and 10 K the sample does not completely saturate. At 10 K the 3 T magnetization is 85.4 emu/g with a 200 Oe coercivity (H_C), and a remanent magnetization (MR) of 14.9 emu/g. At 300 K and 3 T the samples magnetization is 74.4 emu/g with HC < 100 Oe and MR 5.6 emu/g. The room-temperature saturation magnetization is extrapolated from the intercept of magnetization vs $H^{(-1/2)}$ to be 106 emu/g. The hysteresis and remanent magnetization present is consistent with interacting magnetic nanoparticles. With use of the model presented by Hadjipanayis et al.,[14] the magnetization can be calculated for core−shell nanoparticles, provided detailed structural data are available from bulk values. Using the diameters determined from TEM, using the phases from XAS, and assuming bulklike densities, we calculate the magnetization to be 115 emu/g. The saturation magnetization values at 10 K are in good agreement with the magnetic contribution of the core, while extrapolated saturation values are in close agreement with the combined core and shell magnetization.

The 3 T magnetization values were also used to evaluate the effectiveness of the passivating oxide shell. The quality of the coating is presented in magnetization versus time plots as an inset in Figure 3 with the nanoparticles showing only a 10% reduction in the magnetization after 48 days. Previous attempts to synthesize passivated Fe nanoparticles based on core−shell morphology have failed in part due to a lack of comprehensive short-range structural information. The nanoparticles presented here consist of a metallic iron glass surrounded by a disordered oxide shell. This shell protects the metallic core from oxidation for at least 6 weeks.

Acknowledgment. We acknowledge the support of the Office of Naval Research (ONR) and the Defense Advanced Research Projects Agency (DARPA). Scott Calvin is a National Research Council (NRC) research associate at NRL. This research was performed in part at the National Synchrotron Light Source, which is sponsored by the Department of Energy.

Supporting Information Available: Additional experimental details and figure (PDF). This material is available free of charge via the Internet at http://pubs.acs.org.

CM034131L

(10) Calvin, S.; Carpenter, E. E.; Harris, V. G. Unpublished.

(11) Specifically, equal masses of α-Fe_2O_3, γ-Fe_2O_3, Fe_3O_4, and FeOOH. The XANES spectrum of all iron oxides are similar, so the specific oxides chosen were somewhat arbitrary.

(12) Toney, M. F.; Davenport, A. J.; Oblonsky, L. J.; Ryan, M. P.; Vitsu, C. M. *Phys. Rev. Lett.* **1997**, *79*, 4282−4285.

(13) Kerkar, M.; Robinson, J.; Forty, A. J. *J. Faraday Discuss.* **1990**, *89*, 31−40.

(14) Gangopadhyay, S.; Hadjipanayis, G. C.; Dale, B.; Sorensen, C. M.; Klabunde, K. J.; Papaefthymiou, V.; Kostikas, A. *Phys. Rev. B* **1992**, *45*, 9778−9787.